Original Research Article

Numerical lnvestigations of Sloshing Characteristics in Long Moving Vessels with Embedded Concave Rigid-ring Baffle in Gravity Environment

ABSTRACT

Flat Rigid–ring Baffle (FRB) is a common slosh suppression device in Long Moving Vessel (LMV) to mitigate against oscillation-induced instability due to sloshing of its content but, its relative low performance unacceptable for desirable safety standard thus, necessitating continuous efforts to investigate other baffle configurations. Investigation of Concave Baffles of varying geometries was carried out with CFD in a gravity milieu. This work was therefore designed to study the sloshing characteristics of Water-Carrying Cylindrical (WCC) tank equipped with three baffles. Model governing equations based on conservation of mass and momentum were developed and solved using Finite Element Analysis (FEA) technique. The model was used to evaluate Damping Ratio (DR) from Mile's equation at 72, 66 and 59 percent standard positions in a 75 percent filled water-carrying cylindrical vessel with slenderness ratio of 1.5 excited at a frequency of 2 *Hz*. The investigated baffles were Concave Rigid-ring Baffle-1 (CARB1) 0.02 m pitch, Concave Rigid-ring Baffle-2 (CARB2) 0.04 m pitch and Flat Rigid-ring Baffle, FRB (control). Data were presented in term of none dimensional DR and as the main performance index. Numerical results were obtained and compared with FRB results also obtained numerically. The results showed that, the concave baffles exhibited better damping characteristics at 72 and 59 percent water-filled positions of the cylinder which mostly the critical states hence, Concave-Rigid-ring Baffle have better damping effectiveness than Flat-Rigid-ring Baffle.

Keywords: Sloshing, Damping-Ratio, Gravity, Instability, Cylinder.

1. Introduction

Liquid movement in partially-filled storage tank or vessel as a result of its inertial forces induced oscillatory motion from the motion of the container such as stage separation and trajectory correction of a launch vehicle, mostly referred to as propellant slosh, Liquefied Natural Gas (LNG) truck moving on a rough road, water tanker are good examples of the illustration of this phenomenon. Sloshing could be defined as to and fro free surface motion of liquid (ML) in a not-filled to the brim container, due to disturbances by way of perturbations. Liquid response in a container can be analysed or study when attached to a Long Moving Vessel (LMV) such as fuel tanks of aircrafts, Liquid Rocket Engine, ships,

automotive vehicles, etc. Dynamic systems (DS) designer require information from the analysis of this phenomenon for stability and instruments placement. Elastic body frequencies, and the fuel-slosh frequencies must all be reasonably separated, in most cases it is not so. If the dominant fuel-slosh frequencies are close to any of the control system frequencies, an instability in the flight characteristics can result; while if the fuel-slosh frequencies are close to the elastic body bending frequencies, a large amplitude dynamic response problem may arise (Abramson, 1966).

Slosh magnitude is a function of the container geometry, fluid properties, fluid-filled level, perturbing motion of the container, acceleration field and damping capability of the system. Sloshing problem revolves primarily on measurement of hydrodynamic pressure distribution, forces, moments and natural frequencies of the free-liquid surface. To eschew catastrophic sloshing in LMVs, its frequencies must be widely separated from the sloshing-fluid frequencies (Ibrahim, 2005). Non-linear nature of sloshing necessitates the use of Experimental and Computational Fluid Dynamic (CFD) (Eswaran, 2011). The objective of this study is to investigate possible baffle configuration that can reduce vibration-induced sloshing in a LMVs hence, the specific objective is:

Investigation of the effect of Concave Ring-ring Baffles on sloshing characteristics in a LMVs, and the results were compared with a FRB numerically.

II Literature Review

Dou *et al.* (2020) investigated the significant of Tuned Liquid Damper (TLD) in damping non-linear vibration of elastic Supporting Structural Platform (SSP).It was observed that the amplitude of the roof plate reduced appreciably and a frequency shift after TLD on the SSP. Also, energy equilibrium between absorption and production was broken due to abrupt excitation which resulted in larger wave height.

Jing-Han *et al.* (2019) studied sloshing and the effect of vertical baffle attached to the bottom of a tank. Linear Velocity Potential Theory (VPT) was employed in the study. Their conclusion was that, motion of the baffle, both magnitude and phase can be adjusted simultaneously in reducing the Free Surface Elevation (FSE) and significant reduction of sloshing wave.

Chia Chu *et al.* (2018) employed both experimental and numerical simulation to investigate sloshing with embedded multiple baffles fixed at bottom of a rectangular tank containing water. Volume of Fluid (VOF) method was employed in solving free surface

equation. Validation of the simulation results was performed with shaking-table experiment. Determination of the impact of baffle's height and the space between them on slosh suppression was the objective of the study. Simulation results affected the Natural Frequency (NF) of the tank significantly, as a result of the present of multiple baffles. The reduction of the Hydrodynamic Force (HF) by the multiple baffle is much than a single baffle also, forces from the tank's sidewall due to integrated pressure can be represented by Slosh-Wave Amplitude (SWA). Frequency, water depth, Slosh-Wave Amplitude and HF reduced while, baffles height and its numbers increased hence, there was reduction in impact of baffles on slosh suppression when the relative baffle height, i.e., $hb/hw \geq 0.75$.

Mi-AnXue *et al*. (2017) studied four types of baffles and its effectiveness in slosh suppression under a forcing frequencies of *0.4 ω1 to 1.4 ω1*.Effectiveness of the baffle of vertical geometry near the Free surface is significant in slosh suppression than the one fixed at the bottom of the container. Slosh suppression of perforated baffle of vertical geometry is more significant than surface-piercing counterpart of vertical geometry mounted at the bottom of the tank at broad band frequency region. It was observed that the tank-liquid system first-mode NF was changed with the present of the vertical baffles. The result of the experiment showed that alteration of flow fields and NF may significantly damp HF on the tank walls. Compressible VOF was better in obtaining more precise predictions of sloshing.

Zhiqiang *et al.* (2016) in their numerical study showed that Floating Liquefied Natural Gas FLNG-tank motion affected the roll motion response significantly. They also, established that tank fill at moderate level does not reduce roll motion response significantly.

III. Computational Modeling

A concave baffle was selected for numerical set up, dimension was selected to ensure geometrical similarity with the numerical equivalent hence, the concave baffle set up characteristics are listed below:

Baffle focal length: 0.0200 m and 0.0400 m

Tank is 75 % filled with water

Baffle positions: 72%, 66%, 59 % respectively)

Tank size: 0.6 m (height); 0.4 m (diameter).

Figures 1 to 3 show geometry creation using ANSYS CFX Workbench 15.0, SolidWorks 2014 illustration of geometrical representation of Concave Rigid-ring Baffle (CARB1 and CARB2) of 0.1m of thickness. Also, figures 4 shows geometrical representation of Flat Rigid-ring Baffle (FRB) as the control.

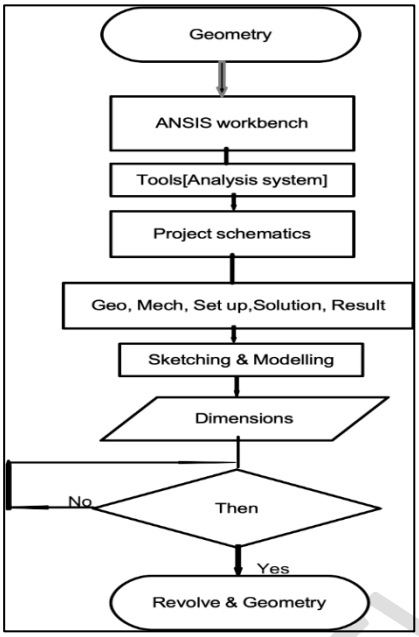

Figure 1**:** Flow-chat illustration of geometry creation. (ANSYS CFX Workbench 15.0 November, 2013)

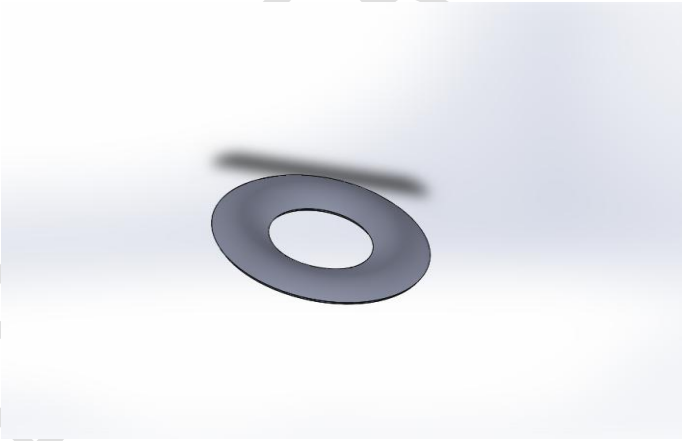

Figure 2: SolidWorks 2014 illustration of Concave Rigid–ring Baffle with pitch of 0.0200 m

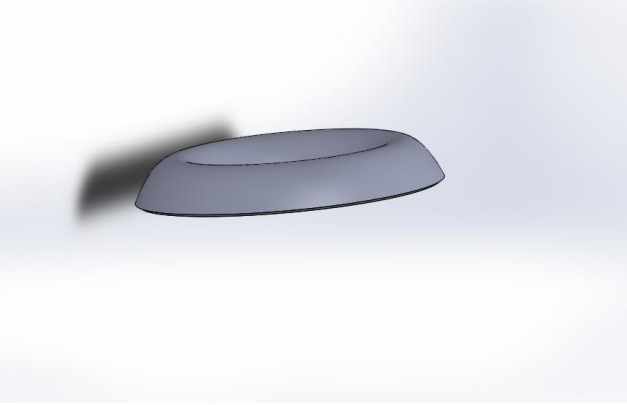

Figure 3: SolidWorks 2014 illustration of Concave Rigid–ring Baffle with pitch of 0.0400 m

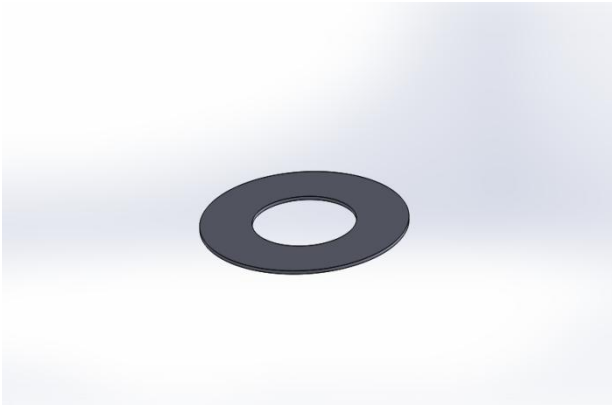

Figure 4: SolidWorks 2014 illustration of Flat Rigid – ring Baffle of 0.1 m width

Figure 5 illustrates a sample of finite element of the tank, baffle and the test fluid (water).

Continuity Equation

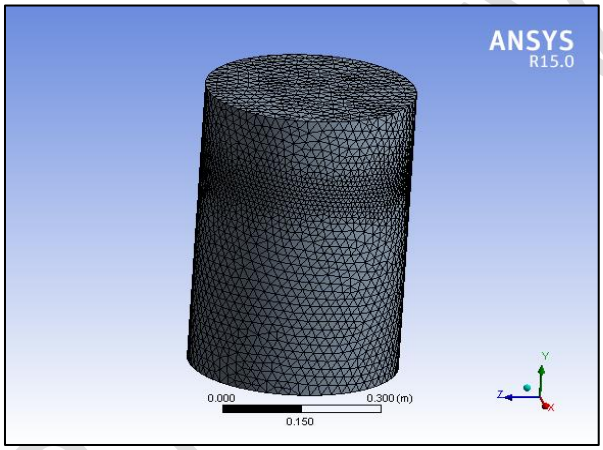

Figure 5: Finite Element Mesh of the Computational Domain (ANSYS Modelling Meshing Guide, 15.0 November, 2013)

Figure 6 shows algorithms for problem set-up.

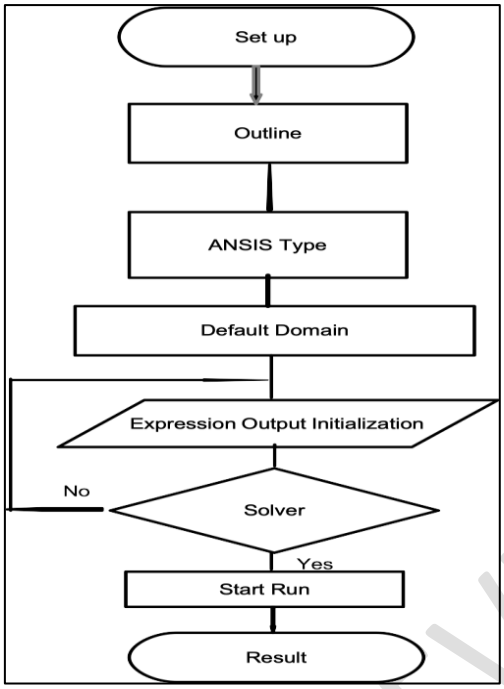

Figure 6 Set-up Algorithm

Equation of Motion

The dynamic of fluid while in motion could be represented mathematically by equations derived from conservation of mass and Navier-Stokes equations, Çengel, Y.A. and Cimbala, J., M. (2006). These equations were solved to obtain pressure and velocity, which were used to evaluate the forces at the walls of the tank. The basic differential equation that a velocity potential must satisfy everywhere in the
liquid volume is the condition of liquid incompressibility, which is given by:

$$\frac{\partial u}{\partial x}+\frac{\partial v}{\partial y}+\frac{\partial w}{\partial z}=0 \qquad (1)$$

This equation is also known as Continuity Equation, where Eq. (2) represents general differential and compressible form of this equation.

$$\frac{\partial \rho}{\partial t}+\vec{V}.\left(p\vec{V}\right)=0 \qquad (2)$$

Where $\vec{V}$ is the component of velocity vector in *x, y, z* axes respectively.

Momentum Equation (incompressible Navier–Stokes equation in vector form)

$$\rho\frac{D\vec{V}}{Dt}=-\vec{\nabla}p+\rho\vec{g}+\mu\nabla^2\overrightarrow{V} \qquad (3)$$

$$\nabla^2=\frac{\partial^2}{\partial x^2}+\frac{\partial^2}{\partial y^2}+\frac{\partial^2}{\partial z^2} \qquad (4)$$

Where, ∇^2 is the Laplacian operator, in Cartesian coordinate, $\vec{g}$ is acceleration due to gravity in vector form.

Integration of these governing equations yields non-steady version of Bernoulli's equation for a potential flow without vorticity as:

$$\frac{\partial \phi}{\partial t} + \frac{p}{\rho} + gz + \frac{1}{2}(u^2 + v^2 + w^2) = f(t) \quad (5)$$

where, *Φ. P, ρ* and *g* are the velocity potential, fluid pressure, fluid density and effective gravity acting in the negative *z* direction (this is equivalent to laboratory value but in opposite direction to the axial acceleration for a space vehicle) respectively. Small values of velocities *u, v, and w* were assumed, for the squared and higher power terms of these values to be negligible in comparison to those terms that are linear for linearization of the equation. Existence of the derivative of the velocity potential with physical meaning facilitates addition of time function to the definition of *Φ*. Hence, constant of integration *f (t)* in Eq. (5) is absorbed into the definition of *Φ,* linearised form of the equation (5) is in the form of Eq. (6), as detailed by Franklin (2000)

hence,

$$\frac{\partial \emptyset}{\partial x} + \frac{p}{\rho} + gz = 0 \quad (6)$$

.

Boundary Conditions (BC) at the Free Surface

The walls BC and FS of the tank could be satisfied by solution of any mathematical function that satisfy equation (1). Also, Equation (6) is used to derive one of the BC at the FS. There is a free movement of the surface hence, insignificant values of the gas density in comparison to the liquid pressure at the surface, makes it equal to gas static pressure p_0 at the FS. Nonsteady Bernoulli's equation at the FS is given by Franklin (2000) in the form

$$\frac{\partial \phi(x,y,z,t)}{\partial t} + g\delta(x,y,t) = \frac{p_0}{\rho},$$

$$\text{for } z = \frac{h}{2} \quad (7)$$

FS small displacement is represented by *δ(x, y, and t)* and the height above FS is given in the form

$$z = h/2 \quad (8)$$

Unlinearised Eq. (7) would be solved at the point of displacement, therefore

$$z = h/2 + \delta \quad (9)$$

of the FS instead of equilibrium position

i.e.

$z = h/2$. The difference between the two conditions *($z = h/2$ and $z = h/2 + \delta$)* results in higher order term of δ, which could be neglected. For small value of g, surface tension effect is significant to be considered in Equation (7). Gas pressure retains its value as p_0 but, pressures values of liquid and gas are not the same at the FS and the adjacent side, this difference is a function of surface curvature and tension. Equation (7) represents the "dynamic" state at the FS. Relationship between displacement at the surface δ and the component of the velocity along vertical axis of the liquid at the FS requires kinematic analysis. In a linearised form, this condition is simply.

$$\frac{\partial \delta}{\partial t} = w = \frac{\partial \varphi}{\partial z} \quad , \quad \text{for} \quad \frac{h}{2} \qquad (10)$$

Combining Equations (7) and (10) and writing it in terms of φ $(or\ \delta)$ and differentiate with respect to *t* and z respectively, combine both equations to eliminate φ $(or\ \delta)$ output to be,

$$\frac{\partial^2 \varphi}{\partial t^2} + \frac{\partial \varphi}{\partial z} = 0 \text{ for } \frac{h}{2} \qquad (11)$$

Natural frequency of the sloshing is an integral part of the time derivative of φ in Eq. (11) which shows a direct relationship to the imposed gravitational field, earlier mentioned.

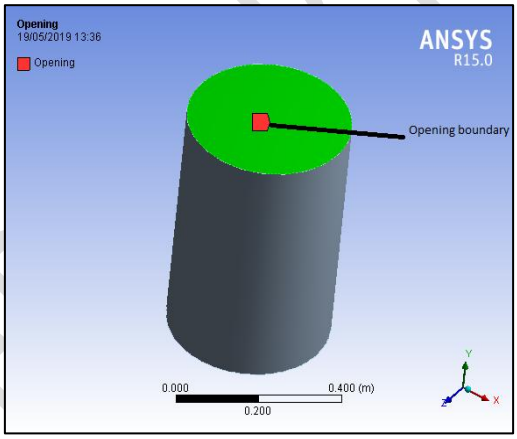

Figure 7: Opening Boundary conditions

Boundary Conditions at the Tank Walls

Assumption of negligible values of viscosity and viscous stresses render these quantities unsuitable for defining boundary condition at the wall hence, the value of velocity perpendicular to the wall's plane of the tank, which is equal to V_n is more appropriate, (*n* stands for normal direction) and condition of "No-slip" is applied. For a stationary tank, the BC at the wall is the normal velocity component of the liquid to the wall and equal to zero. The value represents the standard type of BC value problem. Assumption of oscillation of the liquid, leads to a problem of non-standard boundary value, solvable by employing Fourier series. Non-oscillatory motion of tank that result to none standard problem, transformation

could be done mathematically by representing liquid motion in two parts. Rigid body motion similar to tank's motion, and liquid motion relative to the RB motion. This approach is similar to what is obtainable in solid dynamics to analyse particle's motion relative to a coordinate system in motion as detailed by Franklin (2000) hence, transformation in term of velocity potential is cast in this form;

$$\Phi = \emptyset_c + \emptyset \qquad (12)$$

where Φ is the velocity potential, $\emptyset_c$ and $\emptyset$ are the potential for the tank's rigid body motion and a motion of the liquid relative to the rigid body motion respectively hence, BC for Φ at the wall of the tank's wall reduces to.

$$\frac{\partial \emptyset_c}{\partial n} = V_n \qquad (13)$$

$$\frac{\partial \emptyset}{\partial n} = 0 \qquad (14)$$

Where, V_n is the liquid velocity perpendicular to the plane of the wall, and *n* stands for the normal or perpendicular direction.

This could not be applied to tank in rotational motions as velocity potential of the tank motion would have a non-zero value of vorticity. Sloshing problem is linear hence, it requires solving problems of different tank motion based on their configurations and integrate the results to obtain velocity potential for the whole motion (Franklin, 2000).

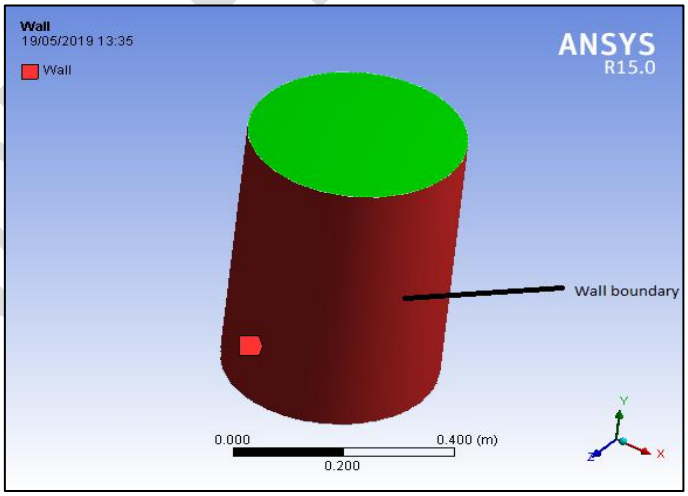

Figure 8: Wall boundary conditions

$$\boldsymbol{F_x} = \sum_{\boldsymbol{c}}^{\boldsymbol{wetted\ area}} \left(\boldsymbol{p_c} * \vec{\boldsymbol{A}}_{\boldsymbol{cx}}\right) \qquad (15)$$

$$\boldsymbol{F_y} = \sum_{\boldsymbol{c}}^{\boldsymbol{wetted\ area}} \left(\boldsymbol{p_c} * \vec{\boldsymbol{A}}_{\boldsymbol{cy}}\right) \qquad (16)$$

$$\boldsymbol{F_z} = \sum_{\boldsymbol{c}}^{\boldsymbol{wetted\ area}} \left(\boldsymbol{p_c} * \vec{\boldsymbol{A}}_{\boldsymbol{cz}}\right) \qquad (17)$$

Equations 15 to 17 are the force application obtained from the force aggregate at the wall of the cylinder.

Miles' equation (Performance Evaluation Index)

For a flat rigid-ring baffle in a cylindrical tank, the damping ratio as a function of baffle depth d should be estimated from Miles' equation. The damping ratio which is a measure of the baffle performance is then estimated from:

$$\xi = \frac{\delta}{2\pi} = 2.83e^{-4.60\frac{d}{R}\left[\frac{2W}{R}-\left(\frac{W}{R}\right)^2\right]^{\frac{2}{3}}}\left(\frac{\eta}{R}\right)^{\frac{1}{2}} \qquad (18)$$

ξ, damping ratio; w, baffle width; η, maximum slosh-wave height at the wall and δ, the damping factor (or logarithmic decrement) and R, tank radius. The term in brackets is the fraction of the tank area covered by the baffle (Miles, 1958).

IV. Comparison of the numerical results.

Figures 9 and 10 are the graphs showing CARB1 and CARB2 respectively, slight appreciation in the values of DR were observed upon pitch increment.

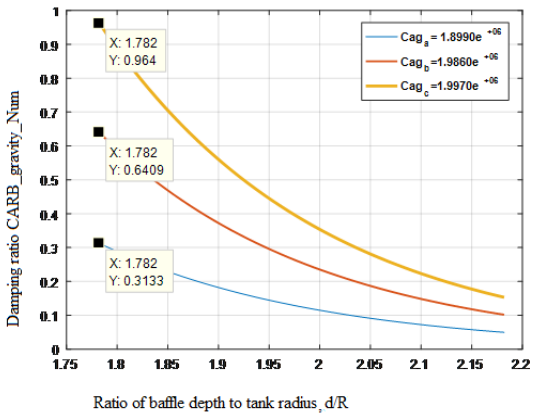

Figure 9: CARB1 graphs showing DR values at different positions of the tank-water depth

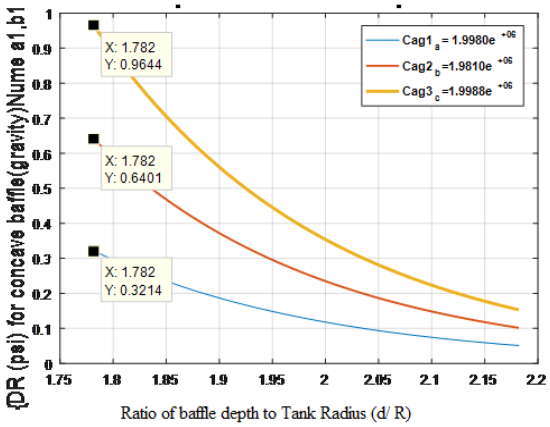

Figure 10: CARB2 graphs showing DR at different positions of the tank-water depth.

Table: 1. Slosh Wave Amplitude, Damping Ratio of CARB1 and CARB2

Baffle Configuration	Slosh-Wave Amplitude	Damping Ratio
CARB 1 0.0200m	1.8990e+06 1.9860e+06 1.9970e+06	0.3133 0.6409 0.9640
CARB 2 0.0400m	1.9980e+06 1.9810e+06 1.9988e+06	0.3214 0.6401 0.9644

Figure 11 and Table 2 are the graph of Damping Ratio and Slosh Wave Amplitude of FRB obtained numerically in gravity environment,

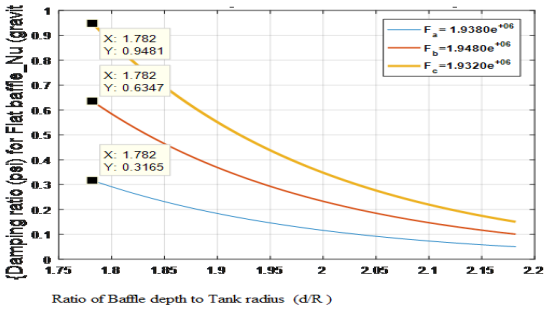

Figures 11. The graph of Damping Ratio for FRB.

Table: 2. Values of Slosh Wave Amplitude and Damping Ratio for FRB

Baffle config-urations	Slosh-Wave Amplitude Numerical	Damping Ratio
FRB Numerical	1.9380e+06 1.9480e+06 1.9320e+06	0.3165 0.6347 0.9481

Tables 1 and 2 show the values of Damping Ratio of CARB1, CARB2 with pitch values of 0.0200, 0.0400m and FRB, secured at 59, 66 and 72 % filled-position of the tank. At 72% baffle position, DRs were: 0.3133, 0.3214, 0.3165, for CARB1, CARB2, FRB respectively. At 66%, DRs were 0.6409, 0.6401, 0.6347 for CARB1, CARB2, FRB respectively. At 59%, DRs were 0.9640, 0.9644, 0.9481 for CARB1, CARB2, FRB respectively. At 72 and 59 percent filled positions of the tank, DR value for the CARB was higher than FRB when the pitch was increased from 0.02m to 0.04m while, the DR of the FRB was slightly higher than CARB when the pitch has not increased. CARB has better damping characteristic than FRB.

(V) Conclusion

Results obtained numerically from concave baffles of varying pitch were compared with FRB, it was found that concave baffle has better damping characteristics than FRB.

References

Abramson, H.N., 1966. The dynamic behaviour of liquids in moving containers with Applications to Space Vehicle Technology NASA SP-106. NASA Special Publication, 106.

ANSYS CFX Reference Guide, November 2013. User's Guide Release 15.0, ANSYS Inc. USA.

ANSYS CFX-Solver Modelling Guide, November 2013. User's Guide Release 15.0, ANSYS Inc. USA.

ANSYS CFX-Solver Theory Guide, November 2013. User's Guide Release 15.0, ANSYS Inc. USA.

Çengel, Y.A. and Cimbala, J., M. (2006). Fluid mechanics fundamentals and applications.

Chia Chu. 2018 .Slosh-induced hydrodynamic force in a water tank with multiple baffles National Central University. Article in Ocean Engineering

Chu CR, Wu YR, Wu TR, Wang C-Y (2018) Slosh-induced hydrodynamic force in a water tank with multiple baffles. Ocean Eng 167:282–292

Eswaran, M. and Saha, U.K., 2011.Sloshing of liquids in partially filled tanks–a review of experimental investigations. Ocean Systems Engineering, 1(2), pp.131-155, pp.198-205.

Franklin T. Dodge 2000 .The new dynamic behaviour of liquids in moving Containers, Southwest Research Institute San Antonio, Texas

Heng Jin, Yong Liu, Ruiyin Song and Yi Liu 2020. Analytical study on the effect of a horizontal perforated plate on sloshing motion in a rectangular tank Journal of Offshore Mechanics and arctic Engineering

Jing-Han Wang and Shi-Li Sun 2019. Study on liquid sloshing characteristics of a swaying rectangular tank with a rolling baffle. Journal of Engineering Mathematics volume 119, pages23–41

M. L. Turner, ''Rocket and Spacecraft Propulsion'', Principles, Practice and New Developments (Second Edition) CBE Department of Physics and Astronomy University of Leicester, UK

Miles, J.W., 1958. Ring damping of FS oscillations in a circular tank. J. Appl. Mech, 25(2), pp.274-276.

NASA Space Vehicle design criteria (Guidance and Control), 2001, pp.36-41, pp.121-125.

Peng D, Mi-AnXue and Jinhai Z., (2020). Numerical and experimental study of tuned liquid damper effects on suppressing nonlinear vibration of elastic supporting structural platform

Release 12.0 c ANSYS, Inc. March 12, 2009

D 715).NATIONAL AERONAUTICS AND SPACE ADMINISTRATION WASHINGTON DC.

Simple and Easy Tutorial on FFT Fast Fourier Transform Matlab Part 1 (1) item type MP4 Video

Simple and Easy Tutorial on FFT Fast Fourier Transform Matlab Part 2(2) Item type MP4 Video. Reynolds Transport theorem

Simple FFT and Filtering Tutorial with Matlab – Code Project

Simulation of kerosene-liquid tank sloshing with baffles using Fluent, MP4 Video

The Focus Video Tips- Multiphysics Simulation with ANSYS Maxwell and ANSYS Mechanical - Part 2 mP4 Video

TUTORIAL 10: Simulation of Multiphase problem with ANSYS CFX-Sloshing in a Tank

Tutorial: Fuel Tank Sloshing ANSYS, Inc. February 9, 2011.

Wang WY, Peng Y, Zhou Y, Zhang Q (2016). Liquid sloshing in partly-filled laterally-excited cylindrical tanks equipped with multi baffles. Appl Ocean Res 59:543–563

Xue, M.A., Zheng, J. and Lin, P., (2012). Numerical simulation of sloshing phenomena in cubic tank with multiple baffles. Journal of Applied Mathematics, 2012.Pp.8-16.